

Self-Organizing OFDMA Systems by Random Frequency Hopping

Markus Putzke and Christian Wietfeld

Communication Networks Institute (CNI)
 TU Dortmund University, 44227 Dortmund, Germany
 {Markus.Putzke, Christian.Wietfeld}@tu-dortmund.de

Abstract—This paper analyzes the use of Random Frequency Hopping to enable self-organizing Orthogonal Frequency Division Multiple Access systems (RFH-OFDMA). While LTE (Long Term Evolution) macrocell resource planning is typically based on centralized planning of orthogonal deterministic frequency hopping patterns, the integration of femtocells located within macrocells introduces either complex planning efforts or uncontrolled interference issues. The results presented in this paper show that random frequency hopping is a new effective way to reduce interference for the integration of femtocells without resource planning into macrocells. An analytical model for the SINR (Signal-to-Interference-and-Noise Ratio) and a simulation model for the BER (Bit Error Rate) are presented for interfering RFH-OFDMA systems. All OFDMA parameters can be freely selected in time and frequency in the model, enabling to dimension systems with minimal interference. Based on the analytical model, a performance evaluation is presented, which uses typical LTE parameters. Compared to the performance of systems without resource planning and random frequency hopping, a significant gain is achieved for self-organizing RFH-OFDMA systems with respect to the SINR and BER.

I. INTRODUCTION

OFDMA based systems are widely deployed nowadays as they offer broadband wireless access with numerous advantages compared to other multiple access technologies [1]. Owing to constantly growing wireless traffic, operators are introducing femtocells to reduce excessive traffic in macrocells and to extend indoor coverage. In this way, capacity bottlenecks can be compensated by providing short-range hot-spots. As a result, higher signal qualities, higher throughputs and lower power consumptions can be achieved. Moreover, higher spatial reuse and enhanced system capacities are possible [2].

Especially user-installed femtocells are often deployed in an uncoordinated way, such that neither the locations nor the used subbands are aligned to the surrounding macrocell. Due to the fact that femtocells operate in the same bands as macrocells, interference between them occurs, cf. Fig. 1. Applying conventional resource planning in form of orthogonal frequency hopping patterns to the femtocells would require a high administrative overhead. Therefore, self-organization techniques are needed, which allow to integrate the femtocells themselves into the macrocells.

Different self-organization techniques have been presented for femtocells. In order to reduce interference, power control

can be used in a way such that the average received power of the macrocell is equal to the power of the femtocell at its cell boundary [3]. Another method is to adjust the power of the femtocells so as to minimize the number of connecting attempts from passing users [4]. For the case of a large number of femtocells, [5] proposes a technique to assign random subsets of frequencies to each cell in order to avoid persistent collisions. Furthermore, the authors in [6] introduced an approach to dynamically tune the femtocell's subchannel allocation based on channel sensing. Since dynamical subchannel allocation for the macrocells or base station coordination in order to avoid interference, we refrain from this method.

In classical resource planning of OFDMA systems, user subbands are changed according to deterministic time-frequency hopping patterns which are orthogonal to each other [7]. Each user allocates its own subband with respect to a certain time slot, so that no interference occurs. Common approaches for orthogonal patterns are Latin squares [7] or truncated Costas sequences [8]. Systems using this centralized resource planning are called Frequency Hopping OFDMA (FH-OFDMA).

In this paper, we propose to replace centralized predetermined patterns by dynamical hopping patterns which are chosen randomly by the femtocell users. Thereby the femtocell is able to integrate itself into the frequency bands of the macrocell with limited interference. That way, the femtocell

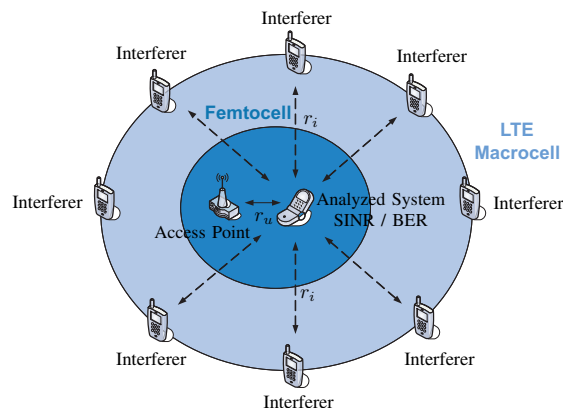


Fig. 1. Analyzed scenario

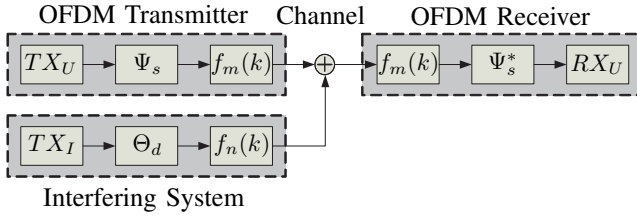


Fig. 2. System model as a block diagram

does not require planning or maintenance by sophisticated centralized methods, but it is self-configuring. Although self-organizing systems are often characterized by the response to their environments, [4] [6] and [9], our approach is capable of handling the integration of the femto- into the macrocell without any exchange of information. Each transmitter chooses a random hopping pattern before transmission according to a given probability density function (pdf) and informs the receiver about the selected pattern. As a consequence, the base station does not need to coordinate patterns as in FH-OFDMA systems, i.e. no resource planning is necessary. Such systems, called Random Frequency Hopping OFDMA (RFH-OFDMA), were introduced in [10]. The authors show that RFH-OFDMA systems can increase the user capacity as these systems allow to occupy the same subcarriers at the same time.

Due to the fact that the predetermined hopping patterns of the LTE macrocell in Fig. 1 are also random from the perspective of femtocell users, we consider interfering RFH-OFDMA systems in the following. The key challenge is to quantify the interference introduced by the random hopping patterns. Existing approaches like [11], [12] and [13] determine the system performance only by simulations and/or without considering the processing of the OFDM in the transmitter and receiver. In order to capture the performance of self-organizing RFH-OFDMA systems, we present an analytical model deriving the SINR and a simulation model obtaining the BER. These models allow to analyze influences of time and frequency parameters like the user bandwidth, the number of subcarriers and the guard time. Regarding these parameters, we focus on typical values of LTE in our analysis. Moreover, the impact of different pdfs for the random patterns is examined, which has not been considered by previous works. In order to quantify the improvements, we compare the results with the performance of systems using an ideal centralized and orthogonal resource planning (FH-OFDMA) and with systems neither using orthogonality nor resource planning.

Since hopping patterns are randomly chosen, the SINR and BER of each user are the same. Therefore, without loss of generality, we can restrict the analysis to a single OFDM system interfered by another OFDM system randomly changing its carrier frequency. The analysis starts with a system model in section II. In section III, an analytical model for the corresponding SINR is derived. Section IV then illustrates the results derived from the analytical and simulation model regarding the performance of the SINR and BER, followed by the conclusions in section V.

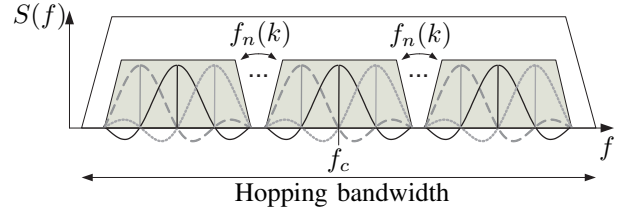


Fig. 3. Realization of frequency hopping

II. SYSTEM MODEL

In this section, the time structure of the transmitted signals, the processing in the receiver and the applied random frequency hopping are introduced in an exact manner. Fig. 2 shows a diagram of the considered system. The OFDM transmitter of the analyzed system consists of a basic modulator TX_U , the orthogonal basis functions Ψ_s and the frequency hopping pattern $f_m(k)$. In contrast, the interfering system uses other basis functions Θ_d and a different hopping pattern $f_n(k)$. The receiver is synchronized to the hopping pattern of the analyzed system $f_m(k)$ and applies conjugated basis functions Ψ_s^* .

A. OFDM Signal Model

According to [14], an OFDM signal can be expressed in the time domain by

$$x(t) = \sum_{l=-\infty}^{\infty} \sum_{d=0}^{N_n-1} z_{d,l} \Theta_d(t - lT_n) e^{j2\pi f_n t}, \quad (1)$$

where N_n is the number of subcarriers, T_n the symbol duration and f_n the carrier frequency. Furthermore, l is the symbol index, d the subcarrier index and $z_{d,l}$ are the transmitted symbols. To ensure the orthogonality between the subcarriers, the basis functions $\Theta_d(t)$ are given by

$$\Theta_d(t) = \begin{cases} \frac{1}{\sqrt{D_n}} e^{j2\pi Q_n d(t - C_n)} & \text{if } t \in [0, T_n] \\ 0 & \text{else} \end{cases}, \quad (2)$$

where C_n is the guard interval due to the cyclic prefix, D_n the data carrying part containing the information and Q_n the subcarrier spacing. Consequently, the OFDM bandwidth is implicitly given by $W_n = Q_n N_n$. Moreover, in order to ensure the orthogonality between the subcarriers, the data carrying part has to be the reciprocal of the subcarrier spacing: $Q_n D_n = 1$. The summation of the guard interval and the data carrying part yields the symbol duration $T_n = C_n + D_n$.

B. Inclusion of Frequency Hopping

According to (1), frequency hopping can be realized by carrier frequencies f_n changing in time. As a consequence, user subbands are shifted, cf. Fig. 3. The time structure of the transmitted signal can then be described as

$$x_H(t) = \sum_{k=-\infty}^{\infty} \text{rect}\left(\frac{t - kT_H}{T_H}\right) x(t) \Big|_{f_n=f_n(k)}, \quad (3)$$

where T_H is the hopping period, $f_n(k)$ describes the hopping pattern and the rect-function is defined as

$$\text{rect}\left(\frac{t}{T}\right) = \begin{cases} 1 & \text{if } t \in [-T/2, T/2] \\ 0 & \text{else.} \end{cases} \quad (4)$$

The hopping period T_H is always greater than the symbol period T_n guaranteeing that at least one symbol is transmitted with a constant frequency.

C. Processing in the receiver

The received signal results from the transmitted signal $x_H(t)$ and the distortion of the channel. In the following, the channel is modeled by a signal attenuation A , which is not necessarily constant over time. Therefore, the interference signal $i(t)$ after down conversion in the receiver can be described by

$$i(t) = Ax_H(t)e^{-j2\pi f_m t}. \quad (5)$$

In order to demodulate the received signal, the baseband processing in the receiver consists of a filter bank matched to the basis functions Ψ_s . Therefore, the impulse response of this filter bank is given by

$$\Psi_s^*(t) = \begin{cases} \frac{1}{\sqrt{D_m}} e^{-j2\pi Q_m s(t-C_m)} & \text{if } t \in [0, T_m] \\ 0 & \text{else.} \end{cases} \quad (6)$$

Without loss of generality, we focus our analysis on the first OFDM symbol in the receiver, as the frequency hopping is applied to each symbol. The interference term after the baseband filtering then becomes, cf. [14]

$$\tilde{i}_s = \int_{C_m}^{T_m} i(t) \Psi_s^*(t) dt. \quad (7)$$

III. ANALYTICAL MODEL FOR SINR

Based on the principles in section II, we determine an exact analysis for the SINR of interfering RFH-OFDMA systems. Beginning with the derivation of the interference signal after demodulation, we introduce a decision variable i_s . With this decision variable, the SINR can be calculated in a straight forward manner.

Since the interference signal after the baseband filtering is given by (7), the use of the transmitted signal (3) and the signal before filtering (5) yields

$$\tilde{i}_s = A \sum_{k=-\infty}^{\infty} \sum_{l=-\infty}^{\infty} \sum_{d=0}^{N_n-1} \frac{z_{d,l}}{\sqrt{D_n D_m}} \beta_{s,d,l,k}, \quad (8)$$

where

$$\beta_{s,d,l,k} = \frac{e^{j2\pi[Q_m s C_m - Q_n d(l T_n + C_n)]}}{j2\pi[Q_n d - Q_m s + f_x]} \times \left(e^{j2\pi U[Q_n d - Q_m s + f_x]} - e^{j2\pi L[Q_n d - Q_m s + f_x]} \right) \quad (9)$$

and the boundaries of the integration are

$$\begin{aligned} L &= \max\{C_m, l T_n\} \\ U &= \min\{T_m, (l+1)T_n\}. \end{aligned} \quad (10)$$

Furthermore, we have introduced the following abbreviation for the difference of the hopping patterns: $f_x = f_n(k) - f_m(k)$.

Without loss of generality, we concentrate on BPSK (Binary Phase Shift Keying) transmitted symbols in the following [14]. These symbols can be demodulated in the receiver by the decision variable

$$\text{Re}\{e^{-j\eta_s} \tilde{w}_s\}, \quad (11)$$

where \tilde{w}_s is the received signal consisting of the signal from the analyzed system \tilde{y}_s , the interference signal \tilde{i}_s and the noise term \tilde{n}_s at the receiver

$$\tilde{w}_s = \tilde{y}_s + \tilde{i}_s + \tilde{n}_s. \quad (12)$$

Furthermore, η_s is the phase of the frequency-domain channel gain of subcarrier s . As a consequence, the interference signal behind the decision circuit can be described as

$$i_s = \text{Re}\{e^{-j\eta_s} \tilde{i}_s\}, \quad (13)$$

which, after inserting (8), results in

$$i_s = A \text{Re}\left\{e^{-j\eta_s} \sum_{k=-\infty}^{\infty} \sum_{l=-\infty}^{\infty} \sum_{d=0}^{N_n-1} \frac{z_{d,l}}{\sqrt{D_n D_m}} \beta_{s,d,l,k}\right\}. \quad (14)$$

In the same manner, we define the decision variables

$$y_s = \text{Re}\{e^{-j\eta_s} \tilde{y}_s\}, \quad n_s = \text{Re}\{e^{-j\eta_s} \tilde{n}_s\}. \quad (15)$$

Since y_s are the symbols of the analyzed system in the receiver, they are given by a multiplication of the magnitude of frequency-domain channel gain g_s and the transmitted symbols $z_{d,l}$ of the analyzed system

$$y_s = g_s z_{d,l} \quad \text{with } s = d + N_m l. \quad (16)$$

Equations (14), (15) and (16) now allow the calculation of the corresponding SNR and SINR in the receiver

$$\begin{aligned} \text{SNR}_s &= \frac{E\{|y_s|^2\}}{E\{|n_s|^2\}} = \frac{E\{g_s^2\}}{\sigma_n^2} \\ \text{SINR}_s &= \frac{E\{|y_s|^2\}}{E\{|i_s|^2\} + E\{|n_s|^2\}} = \frac{E\{g_s^2\}}{\sigma_{i,s}^2 + \sigma_n^2}, \end{aligned} \quad (17)$$

where E indicates the expectation, σ_n^2 the variance of the AWGN (Additive White Gaussian Noise) and $\sigma_{i,s}^2$ the variance of the interference signal per subcarrier. Note that the SINR as well as the SNR are functions of the subcarrier s . If path loss L is constant over time, we obtain

$$g_s^2 = A^2 = L^{-1} = \left(\frac{c}{4\pi f r}\right)^2 \frac{1}{r^\gamma}, \quad (18)$$

where c is the speed of light, r the distance between the transmitter and receiver and γ the path loss coefficient. Utilizing (14), (17) and (18) the variance of the interference signal results in

$$\sigma_{i,s}^2 = A^2 E\left\{\text{Re}^2\left\{\sum_{k=-\infty}^{\infty} \sum_{l=-\infty}^{\infty} \sum_{d=0}^{N_n-1} \frac{z_{d,l}}{\sqrt{D_n D_m}} \beta_{s,d,l,k}\right\}\right\}. \quad (19)$$

As the symbols are stochastically independent and the hopping period T_H is greater than the symbol periods T_m and T_n , the variance $\sigma_{i,s}^2$ becomes independent of the frequency hopping index k

$$\sigma_{i,s}^2 = \frac{A^2}{D_n D_m} \sum_{l=-\infty}^{\infty} \sum_{d=0}^{N_n-1} E \{ \text{Re}^2 \{ \beta_{s,d,l,0} \} \}. \quad (20)$$

In order to calculate the resulting SINR, the variance of the interference per subcarrier has to be averaged over the number of subcarriers, cf. (17)

$$\text{SINR} = \frac{E \{ g^2 \}}{\sigma_i^2 + \sigma_n^2} \quad \text{with} \quad \sigma_i^2 = \frac{1}{N_m} \sum_{s=0}^{N_m-1} \sigma_{i,s}^2. \quad (21)$$

This relationship covers the SINR of two random frequency hopping OFDM systems. In order to get the SINR of M interfering users within a RFH-OFDMA system, we have to replace the bandwidths W_n and W_m by the user subbands. Furthermore, since the interference signals from different users are uncorrelated, we have to multiply σ_i^2 by the number of users M within the macrocell. M is determined as the number of non overlapping subbands fitting into the channel bandwidth minus the bandwidth of the femtocell users. By inserting (18) and (20) into (21) we find

$$\text{SINR} = \frac{1}{\frac{M(r_u/r_i)^\gamma}{D_n D_m N_m} \sum_{s=0}^{N_m-1} \sum_{l=-\infty}^{\infty} \sum_{d=0}^{N_n-1} E \{ \text{Re}^2 \{ \beta \} \} + \frac{1}{\text{SNR}}}, \quad (22)$$

where the indexes of $\beta_{s,d,l,0}$ are omitted for simplicity, r_u denotes the distance from the analyzed system to the access point and r_i the distance to the interferer, cf. Fig. 1. In the case that no frequency hopping is applied, i.e. when $f_n(k) = f_m(k)$, (22) reduces to the result obtained in [14].

IV. RESULTS AND PERFORMANCE ANALYSIS

In this section, we evaluate the performance of interfering OFDMA systems using random frequency hopping. Based on the presented analysis, the SINR as well as the BER are analyzed and compared to systems using an orthogonal resource planning (FH-OFDMA) as well as systems without resource planning and random hopping. As mentioned above orthogonal resource planning is only possible by centralized predetermined patterns. For all following considerations, we assume a number of interferers within the LTE macrocell such that each subband is allocated by a single user, but that no band

TABLE I
SYSTEM PARAMETERS

PARAMETER	VALUE
N_n, N_m	120 subcarriers
W_n, W_m	1.8 MHz
C_n, C_m	$0.25 N_n / W_n$
T_n, T_m	$1.25 N_n / W_n$
Q_n, Q_m	15 KHz
SNR	10
γ	3.5

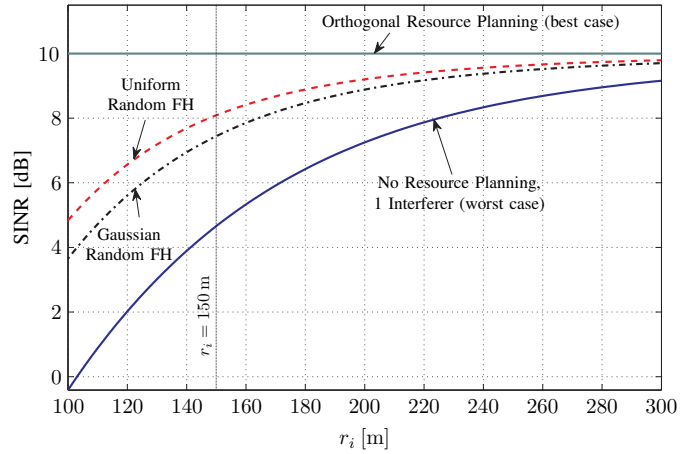


Fig. 4. SINR versus distance of the interfering systems with different frequency hopping distributions and a channel bandwidth of 5 MHz

is assigned to a femto- and macrocell user simultaneously. Subject to that, all results represent a lower bound for the performance of RFH-OFDMA systems. We choose the typical LTE parameters of Table I for evaluation, which are based on [15] and a utilization of 10 resource blocks for all users within the cells. For a realistic scenario, the path loss coefficient is set to $\gamma = 3.5$ which characterizes an urban environment.

Fig. 4 shows the SINR as a function of the distance r_i to the interferers of the LTE macrocell, while the distance between the access point of the femtocell and the analyzed system is constant $r_u = 100$ m, cf. Fig. 1. All users in the femto- and macrocell use the same set of parameters. As can be seen, all curves tend to 10dB for increasing distances r_i , as for large distances the noise power dominates the interference power and the SINR reduces to the SNR. Ideal resource planning with orthogonal separation of the users introduces no interference, so that FH-OFDMA systems always achieve the best performance. In contrast, the worst performance is given by cells without resource planning and random hopping, i.e. cells where all users can permanently transmit in the same frequency subband, cf. Fig. 4.

The dashed line is the result of uniform frequency hopping, where the carrier frequencies are chosen with equal probability from the channel bandwidth, while the semi-dashed line is obtained by a Gaussian pdf. For a fair comparison, the variance σ_G of the Gaussian pdf is chosen such that the interval $\pm 3\sigma_G$ corresponds to the channel bandwidth. As can be seen in Fig. 4, the uniform pdf achieves a higher SINR than the Gaussian one and has a maximum improvement of 5.3 dB compared to systems without resource planning and with one interferer (which is the maximum number of interferers when considering one femtocell user within 5 MHz). The reason is that uniform frequency hopping uses the whole channel bandwidth for transmission, while Gaussian hopping prefers the center of the channel for all transmissions. It can be shown that Gaussian hopping results in less improvement than the uniform one for all channel bandwidths. Therefore, the Gaussian distribution is omitted in all following considerations.

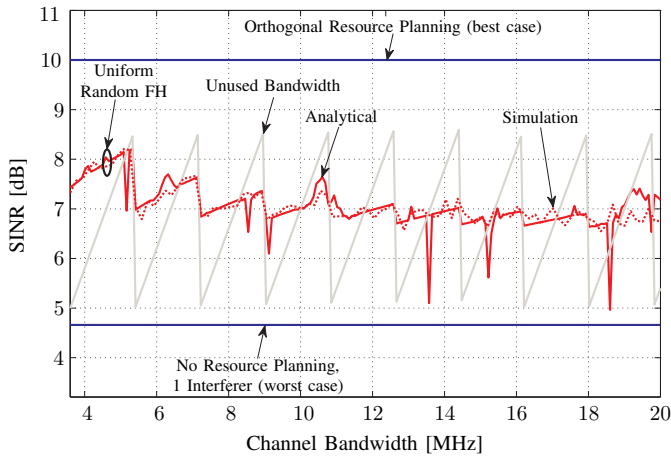


Fig. 5. SINR versus frequency hopping bandwidth using a uniform random hopping distribution ($r_i = 150$ m)

A. Channel bandwidth

The dependency of the hopping gain from the channel bandwidth can be seen in Fig. 5. In this Fig., the SINR at a distance of $r_i = 150$ m is shown for an increasing channel bandwidth, cf. also vertical line in Fig. 4. Note that a rising channel bandwidth results in more interferers, since the bandwidth per user is constantly 1.8 MHz. Hence the unused bandwidth, which is the difference between the channel bandwidth and occupied bandwidth of all users in the cells, is given as a sawtooth function. This free bandwidth cannot be used by cells with centralized resource planning, but is used by systems with random frequency hopping. Therefore the curves for uniform random frequency hopping show a shape according to this sawtooth function. As the SINR of systems without random hopping is independent of the channel bandwidth if the number of interferers is constant, the corresponding curves are horizontal. As can be seen, the best performance of random frequency hopping is 3.5 dB above systems without resource planning and with one interferer, and 1.8 dB below systems with orthogonal resource planning.

All results in Fig. 5 are verified by simulations implemented in MATLAB (dotted curves). The used simulation model comprises an OFDM transmitter generating random bits according to a BPSK, performing an inverse fourier transformation, adding a cyclic prefix and transmitting the resulting signal with a random carrier frequency according to the given pdf of the frequency hopping. Afterwards the signal is attenuated according to the path loss before the symbols are demodulated in the receiver by another random carrier frequency. The resulting random but uncorrelated BPSK symbols of all interferers are added in the receiver to the symbols from the analyzed system, cf. Fig. 1.

B. Number of subcarriers

Next the parameters of the interferers are varied for a constant channel bandwidth of 15 MHz, a constant distance of $r_i = 150$ m and a uniform hopping distribution. In Fig. 6, the number of subcarriers N_n is changed, while $N_m = 240$.

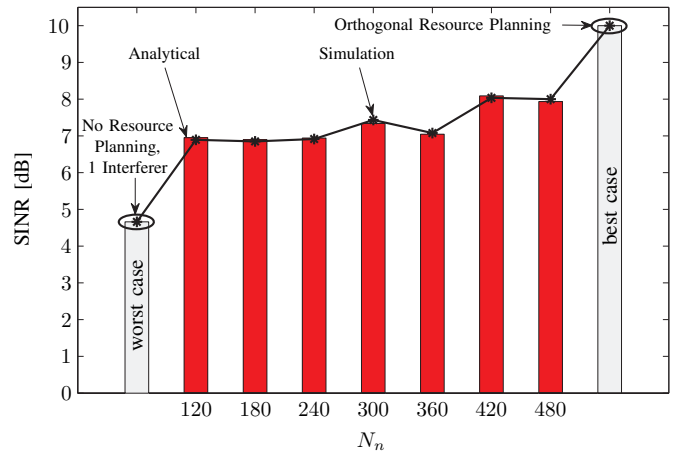


Fig. 6. SINR versus number of subcarriers of the interfering systems using a uniform random hopping distribution ($r_i = 150$ m, $N_m = 240$)

This is equivalent to changing the bandwidth of each interferer, as the spacing between the subcarriers is constantly 15 KHz. A reason for increasing the bandwidth of an LTE interferer, i.e. utilization of more resource blocks, could be a raised Quality of Service requirement within the macrocell like a higher throughput or smaller error rate. Fig. 6 shows that the frequency hopping gain again changes according to the unused bandwidth. As the magnitude of the sawtooth function in Fig. 5 increases with the bandwidth per interferer, the frequency hopping gain increases with the number of subcarriers. Due to the sawtooth character, the gain does not increase in a monotonous way, as we get a little drop for $N_n = 360$. All results are again validated by simulations.

C. Guard time

A similar effect can be achieved when the guard time of the interferers C_n is modified, while the symbol duration T_n remains unchanged, shown in Fig. 7. As these conditions result in a variation of the data carrying part and hence in a variation of the bandwidth per interferer, the unused bandwidth changes in a similar way as it does in Fig. 6. The larger

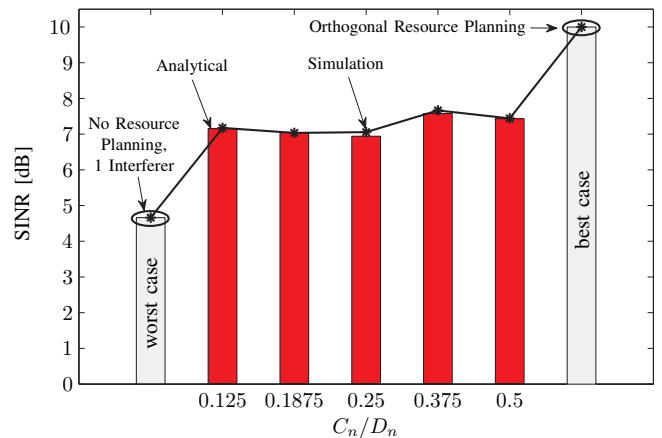


Fig. 7. SINR versus different guard times of the interfering systems using a uniform random hopping distribution ($r_i = 150$ m, $N_n = N_m = 240$)

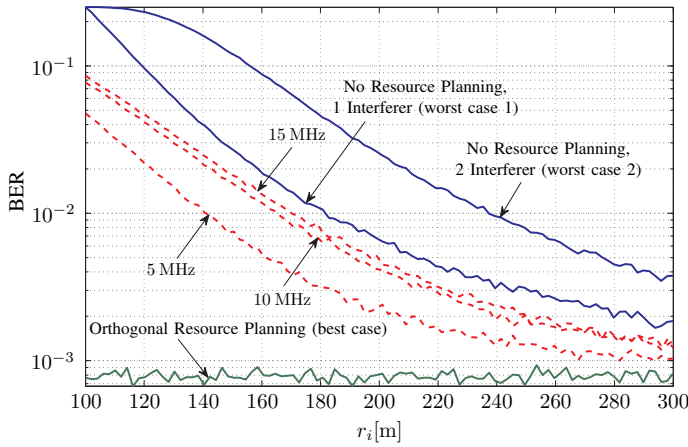


Fig. 8. BER versus distance r_i and channel bandwidth, using a uniform random hopping distribution, derived by simulations ($N_n = N_m = 120$)

the guard time, the smaller the data carrying part and the larger the interferer bandwidth. For this reason, the frequency hopping gain increases in the same way as for the variation of the number of subcarriers. Therefore, the best performance is reached for a guard time of $0.375D_n$ with a frequency hopping gain of 2.9 dB. Fig. 7 shows that the difference between analytical and simulation results is again rather small for all guard times.

D. Bit Error Rate

Finally, we consider the corresponding BER of a uniform frequency hopping OFDMA system. In accordance with the analytical model in section III, the BER per subcarrier s can be determined by the probability that the received symbol is in the different half plane than the transmitted one

$$\text{BER}_s = \frac{1}{2} \text{Prob} \left\{ \left| \text{Re} \left\{ \sum_{m=1}^M i_s + n_s \right\} \right| > g_s \right\}. \quad (23)$$

In order to get the overall BER, (23) has to be averaged over the number of subcarriers N_m . In this way we get Fig. 8, where the BER is depicted as a function of the distance r_i with the channel bandwidth as a parameter. It can be seen that the random frequency hopping gain of the BER shows the same character as for the SINR: the gain increases with the unused bandwidth. The lower the channel bandwidth, the higher the unused bandwidth and the higher the gain. Therefore, the lowest BER is achieved for a channel bandwidth of 5 MHz. For large distances r_i , the interference power disappears, so that all curves tend to the BER for orthogonal resource planning, which is only influenced by the noise. If the channel bandwidth is increased, the same is true for the number of interferers, which results in a higher BER for RFH-OFDMA systems as well as systems without resource planning.

V. CONCLUSION

Since femtocells are used for short-range hot-spots, they are often positioned within macrocells. As they are operating in frequency licensed bands, interference is caused between

femto- and macrocells. An effective way of self-organized integrations for femto- into macrocells is random frequency hopping, where each femtocell user chooses its own random hopping pattern according to a given probability density function. We have presented an analytical model for the SINR and a simulation model for the BER of interfering RFH-OFDMA systems. The performance analysis shows that with respect to parameters of LTE, frequency hopping can achieve a gain of the SINR up to 5.3 dB and a reduction of the BER by a factor of 8. Moreover, we have shown that uniform frequency hopping is more effective than the Gaussian one. The gain of random frequency hopping has been analyzed as a function of the distance, hopping bandwidth, number of subcarriers and guard time. All results show that the potential for improvement depends on the difference between the channel bandwidth and the bandwidth occupied by all users in the cells. Future work will include the analysis of the proposed RFH-OFDMA scheme for more complex scenarios with corresponding frequency-selective channel models and the impact of different service types for the users.

ACKNOWLEDGMENT

Part of the work on this paper has been supported by Deutsche Forschungsgemeinschaft (DFG) within the Collaborative Research Center (SFB 876) "Providing Information by Resource-Constrained Analysis", sub-project A4.

REFERENCES

- [1] H. Yin and S. Alamouti: *OFDMA: A Broadband Wireless Access Technology*, IEEE Sarnoff Symposium, Princeton, Mar. 2006
- [2] V. Chandrasekhar and J. Andrews: *Femtocell networks: A survey*, IEEE Communication Magazine, Vol. 46, No. 9, Sep. 2008
- [3] H. Claussen, L. Ho and L. Samuel: *An overview of the femtocell concept*, Bell Labs Technical Journal, Vol.3, No.1, May 2008.
- [4] H. Claussen, L. Ho and L. Samuel: *Self-optimization coverage for femtocell deployments*, WTS, Pomona, Apr. 2008
- [5] V. Chandrasekhar and J. Andrews: *Spectrum allocation in two-tier networks*, IEEE Transactions on Communication, Vol. 57, No. 10, 2009
- [6] D. Lopez-Perez, A. Ladanyi, A. Jüttner and J. Zhang: *OFDMA femtocells: A self-organizing approach for frequency assignment*, PIMRC, Tokyo, Sep. 2009
- [7] K. Stamatiou and J. Proakis, *A Performance Analysis of Coded Frequency-Hopped OFDMA*, WCNC, New Orleans, 2005
- [8] S. Maric and O. Moreno, *Using Costas Arrays to Construct Frequency Hop Patterns for OFDM Wireless Systems*, Conference on Information Sciences and Systems, Princeton NJ USA, Mar. 2006
- [9] G. de la Roche, A. Ladanyi, D. Lopez-Perez, C. Chong and J. Zhang, *Self-Organization for LTE Enterprise Femtocells*, Globecom, Miami, 2010
- [10] M. Wahlqvist, C. Östberg, J. van de Beek, O. Edfors and P. Brjesson, *A Conceptual Study of OFDM-based Multiple Access Schemes*, Telia Research, Lulea, Sweden, 1996
- [11] Z. Kotic, I. Maric and X. Wang, *Fundamentals of Dynamic Frequency Hopping in Cellular Systems*, IEEE Journal on selected areas in communications, Vol. 19, No. 11, Nov. 2001
- [12] B. Jung and D. Sung, *Random FH-OFDMA System Based on Statistical Multiplexing*, VTC, Stockholm, June 2005
- [13] X. Su, T. Lv, P. Gong, X. Yun and S. Yang: *Multi-Group Frequency Hopping OFDMA Based on Statistical Multiplexing*, IWCMC, Crete Island, Aug. 2008
- [14] C. Snow, L. Lampe and R. Schober: *Impact of WiMAX Interference on MB-OFDM UWB Systems: Analysis and Mitigation*, IEEE Transactions on communications, Vol. 57, No. 9, Sep. 2009
- [15] 3GPP TS 36.211, v. 10.2.0: *Physical Channels and Modulation (Release 10)*, Jun. 2011